Astron. Astrophys. 326, 501–504 (1997)

ASTRONOMY
AND
ASTROPHYSICS

Gas kinematics of the z = 3.8 radiogalaxy 4C 41.17 with TIGER/CFHT⋆

G. Adam[1], **B. Rocca-Volmerange**[2,3], **S. Gérard**[2], **P. Ferruit**[1], **and R. Bacon**[1]

[1] C.R.A.L., Observatoire de Lyon, F-69561 St-Genis-Laval Cedex, France
[2] Institut d'Astrophysique de Paris, CNRS, 98bis Bd Arago F-75014 Paris, France
[3] Université Paris XI, I.A.S., Bat 121, F-91405 Orsay Campus, France

Received 11 July 1996 / Accepted 18 February 1997

Abstract. This paper presents the Lyα1215 Å image, the velocity and velocity dispersion maps of the radiogalaxy 4C 41.17 (z = 3.8), obtained with the integral field spectrograph TIGER at CFHT. In a relatively short exposure time (1.86 h), the Lyα image reveals a bended elongated component surrounding a narrow bright peak and a West fainter component distributed along the radio axis. Roughly perpendicular to that main axis, a South-East to North-West faint extension to the central region is visible. A high density of smaller ionised clouds shows up in the vicinity of the radiogalaxy. The radial velocity and the velocity dispersion are mapped with a 0.61" spatial sampling. Radial velocities, from 0 to 700 km s^{-1}, are essentially negative relative to the narrow peak, while velocity dispersions vary from 800 km s^{-1} in the inner part up to 2000 km s^{-1} at possible bow shock locations as well as in the South extension. Such data are essential to disentangle the various components of these distant sources. The kinematics, roughly similar to that of nearby galaxies, is interpreted by luminous clouds and a dusty disk structure. Measured negative velocities could be used as expansion rate constraints for hydrodynamics models of the radio jet propagation. They may also be due to an overestimate of the systemic velocity, in the hypothesis of a collapsing bright knot at the central bright peak. Information on star formation triggering along the radiojet will be derived from deeper observations.

Key words: galaxies: evolution; intergalactic medium; kinematics and dynamics; jets

1. Introduction

Radiogalaxies are fascinating targets to follow, up to a 90% look-back time, the evolution of galaxies in relation with the central active nuclei and the intergalactic environment. Such studies are difficult, owing to the complex structure of these distant objects. A 3D-spectroscopy of the radiogalaxy field is able to disentangle the various components, allowing independent analyses of their evolution. In that field, 4C 41.17 is a remote radio source till now considered as a template for primeval stellar population studies. The optical/infrared counterpart was discovered at z = 3.800 ±0.003 (Chambers et al, 1990, hereafter CMB) by long slit (4'4×2"5) spectroscopy along the radio axis. A detailed multi-frequency radio analysis (Carilli et al., 1994, hereafter COH) has been made with the V.L.A. and MERLIN, allowing to delineate the fine radio structure of the galaxy in relation with its optical structure. High spatial resolution red continuum (≃1460 Å in the galaxy rest frame) morphology was obtained with the HST (Miley et al., 1992, hereafter MCBM) over a 3 arcsec^2 field. Keck observations (Graham et al, 1994) show strong contributions of the [OIII] and Hβ lines to the K-band flux. From a low spatial resolution velocity field, obtained at Calar Alto with a Perot-Fabry instrument, Hippelein and Meisenheimer (1993, hereafter HM) explain the absorption detected in the galaxy spectrum by a foreground cloud. To complete the multispectral study, a submillimetric emission discovered with the JCMT (Dunlop et al., 1994) and IRAM (Chini and Kruegel, 1994) was attributed to a large dust component, related with the foreground cloud. A recent WHT imaging of the field below the Lyman continuum wavelength (Lacy and Rawlings, 1996), using near-UV detectors, shows a high density of possible companion galaxies in the immediate vicinity.

Our observations presented in Sect. 2 enlighten with a better resolution the galaxy kinematics profiled by these previous observations. The image rebuilt from the ≈400 spectra, is presented in Sect. 3. The kinematics (velocity and velocity dispersion) of the gas, as derived from the Lyα emission line, is presented in the same section, while Sect. 4 gives a preliminary interpretation of these data.

2. The observations

The radiogalaxy has been observed with the integral field spectrograph TIGER (Bacon et al, 1995), installed at the 3.60m CFHT. The exposure time, under excellent seeing conditions

Send offprint requests to: G. Adam, ga@obs.univ-lyon1.fr

⋆ Based on observations collected at Canada-France-Hawaii Telescope, which is operated by CNRS of France, NRC of Canada, and the University of Hawaii.

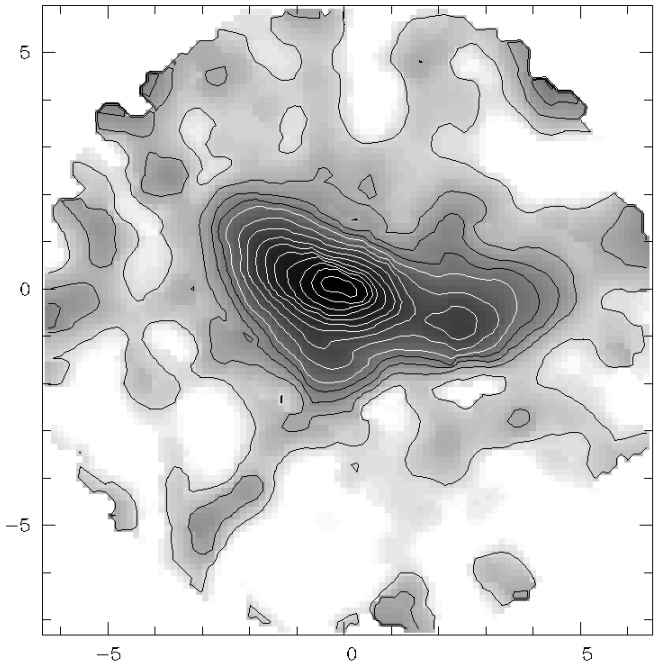

Fig. 1. The Lyα 1215 Å image of the radiogalaxy 4C 41.17 and its environment, reconstructed from individual spectra. North is up and East left; the image has been smoothed with a 0.8″ fwhm gaussian filter. Scale units are arcseconds, and the greyscale is logarithmic. The black contours run from 8% to 20%, with a 4% step, the white ones from 24% to 94% with a 8% step. The (0,0) point indicates the Lyα peak of a brightness 6.5×10^{43} erg s^{-1} arcsec^{-2}, that is 100%.

($\leq$0.5″), was unfortunately limited to 1.86 h by weather conditions. The LORAL3 blue enhanced CCD was used with a 6090 Å / 2430 Å filter. The spatial sampling, i.e. the microlens size, was 0.61″. The data reduction has been performed using the specific TIGER software (Rousset, 1992). The wavelength calibration was done with our Perot-Fabry unit; the [OI] 5577 Å night sky line was used to check its accuracy ($\pm$2 Å), the effective spectral resolution (17.5 Å), and to correct any spectrum-to-spectrum PSF variation. As Lyα emission clouds show up on the whole field, precise absolute astrometry is not easy; we estimate our errors to be $\pm$0.6″ on positions and $\pm5^o$ on position angles. Flux calibration used observations of the standard star Feige 25, and integrated fluxes were derived by summation over spectra with sufficient S/N ratio after redshift correction.

3. Results

3.1. The Lyα image

Fig. 1 presents the Lyα line emission observed over the total 12″$\times$12″ field. For each individual spectrum with S/N ratio $>$2, the Lyα energy is derived from a gaussian fit. The S/N ratio reaches up to 30 on the peak and its near environment and down to 2 to 5 on the surrounding clouds. In the following, we shall adopt $H_0 = 75$ km s^{-1} Mpc^{-1}, $q_0 = 0.5$, the cosmological constant beeing taken as null (1″ = 4.4 kpc). Several structures are identified. A bright Lyα peak, elongated over two spatial elements (2.7×5.4 kpc^2) has a luminosity of 4.8×10^{43} erg s^{-1} with a surface brightness three times higher than in the rest of the galaxy. Around the peak, the main galaxy component has a total luminosity of 2.8×10^{44} erg s^{-1}, while a fainter (7.1×10^{43} erg s^{-1}) secondary component appears to the West. The alignment of the central parts of the two components corresponds to the radio axis (as defined by CMB and COH) between the corresponding radio components B1 and B2/B3. A curvature of the Lyα isophotes towards North-East is clearly visible.The final rotation angle relative to the central radio axis is $\approx20^o$ while MCBM only noted a 7^o change over the HST field of view.

A South-East extension is clearly visible on the main component, roughly coincident with the continuum (R and K) extension seen in Graham et al. (1994). The very central parts of this extension are also conspicuous on the WFPC1 exposures from 1993 HST archives, although the corresponding F569W filter is only transmitting 60% of Lyα. These HST data, despite a poor S/N ratio, show also that the Lyα peak is quite sharp, but do not permit to say if it is resolved or not. The elongation extends faintly towards North-West, possibly tracing the gaseous disk suggested by CMB.

The optical counterpart of this radiogalaxy, including the two components, corresponds to 17.11 arcsec^2 with a total luminosity of 3.8×10^{44} erg s^{-1} and a mean surface brightness of 2.2×10^{43} erg s^{-1} arcsec^{-2}. This total emissivity is in excellent agreement with CMB data. From the rest of the image with S/N $\geq$ 2, ($\approx$90 spatial elements), the radiogalaxy appears to be embedded in an inhomogeneous envelop of Lyα clouds, included in the integrated luminosity of 5×10^{44} erg s^{-1}.

3.2. The velocity field

Fig. 2 presents the radial velocity field of the Lyα gas relative to the peak. The most surprising result is that absolute values of velocities projected along the line of sight are low, i.e. less than 700 km s^{-1}. These values are quite comparable to the gas velocities observed at low redshifts (van Breugel et al, 1985), the signatures of a few thousands km s^{-1} found by CMB from long slit observations beeing undetected. The velocities are essentially negative, giving specific constraints on the gas expansion rate in the surrounding intergalactic medium, or making questionable the adoption of the bright peak redshift (z=3.800) as systemic.

The spatial resolution of the velocity field allows to identify the highest absolute values (-660 km s^{-1} $\geq$V$\geq$-720 km s^{-1} at the North-East and West ends) as possible traces of the radiojet interaction with the intergalactic medium. The West velocity peak is coincident with the West brightness peak, and with the B1 radio spot. However bright hot spots as strong as in 3C435A at z = 0.374 (Rocca-Volmerange et al, 1994) are not detected on the Lyα image.

A zone of regular isovelocity contours, from -250 to -350 km s^{-1} is observed between the two aligned components.

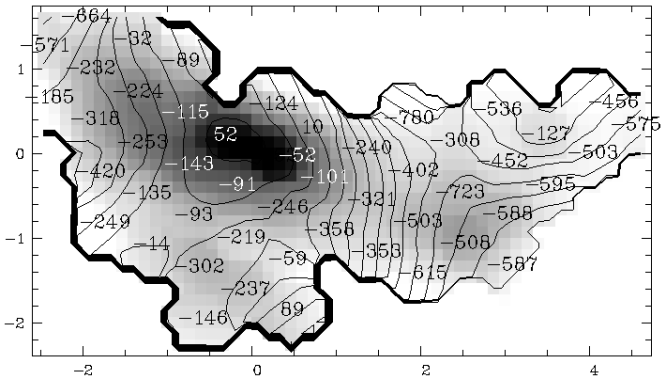

Fig. 2. The velocity field superimposed to the Lyα image. Numbers display radial velocities of individual TIGER spatial elements, in km s^{-1} relative to the Lyα peak value at z=3.800. Isovelocity contours are traced from -650 to 0 km s^{-1}, with a 40 km s^{-1} step. The error (calibration + fit, the former strongly dominant) is $\pm$100 km s^{-1}

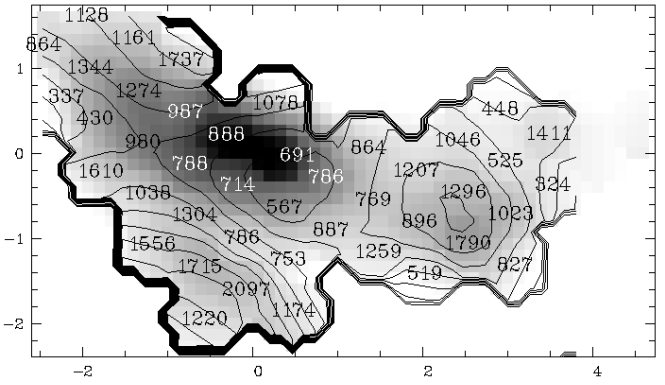

Fig. 3. The velocity dispersion map superimposed to the Lyα image. Numbers display velocity dispersions of individual TIGER spatial elements, in km s^{-1}. Isovalues are traced from 300 to 1700 km s^{-1} with a 100 km s^{-1} step.

More or less perpendicular to the general radio/optical axis, it is roughly located on the South-East to North-West Lyα extension (Sect. 3.1). The S/N ratio is not sufficient in the external parts of the galaxy to identify definite evidences of rotation, but the south extension rotating around the general axis cannot be ruled out from the systematically lower velocities and the shape of the isovelocity contours. Last, we may witness the last stages of a large scale accretion process. Longer exposure times are needed before more definite conclusions.

3.3. The velocity dispersion map

In Fig. 3, the velocity dispersions of the Lyα emission line are superimposed onto the Lyα image. The Lyα line of each spectrum has been fitted by a gaussian and the derived fwhm is used here, after corrections for redshift and instrumental effects. The values are in km s^{-1} in the galaxy rest frame. The velocity dispersions in the central zone, including the peak as well as the area between the two main Lyα components, are $\approx$700-800 km s^{-1}. Higher values of $\approx$1200-2000 km s^{-1} are observed where velocities are the most negative, consistent with the interpretation of the radiojet interaction with the IGM. A second zone of high velocity dispersion appears in the South-East extension.

4. Preliminary analysis

The morphology and gas kinematics of the z=3.8 radiogalaxy 4C 41.17, traced by the Lyα1215Å emission line from TIGER observations, roughly confirm previous results (CMB; HM). However new results are derived from the numerical values of velocities:

i) The two bright zones of the main galaxy body, one including a strong peak, are located along the radio axis; they show moderate (absolute values lower than 700-800 km s^{-1}) negative velocities relative to the peak. The simplest interpretation is that, in the local rest-frame, the all-negative velocities trace a gaseous expansion, as described in classical models of radiojet propagation. However the shock-induced ionisation process associated with the expansion of the radio lobes, according to overpressured cocoon models confined by either ram pressure (Loken et al, 1992) or magnetic effect (Begelman and Cioffi, 1989), is not observed. No evidence of a systematic increase of Lyα velocity dispersion appears along the external limits of the gaseous envelop; the Lyα emission itself is regularly decreasing. Last, this solution relies on the choice of the peak velocity as the systemic one. The strong Lyα peak appears as a bright knot due to the interaction of the radiojet with the inhomogeneous environment. In that case, the peak could be submitted to a strong collapse, and would display a positive velocity relative to the galaxy as a whole.

ii) Velocities are surprisingly low and similar to values observed in nearby radiogalaxies. They do not evoke a powerful dynamical processes triggering an enormous starburst as suggested by various authors. An interesting point is that the Lyα isophotes of the main component present a 20^o bending; that extends further towards North-East the inner radiojet curvature, observed in both the optical and radio domains (MCBM; COH). The bending is an evidence against ionisation by the central AGN, and confirms that the ionized gas intimately follows the radio plasma. Among the main sources of gas ionisation proposed by various authors, dust scattering (di Serego Alighieri et al, 1993), photoionisation by a central engine (van Breugel et al, 1985) or interaction with cosmic background photons (Daly, 1992), the bending favors the theory of star formation triggered along the radiojet, to be confirmed by HST observations.

iii) A dark zone is identified between the two main galaxy components. Characterised by regular isovelocity contours and low velocity dispersions, its kinematics could trace the gaseous disk suggested by CMB. Dust would then explain this Lyα weakening, as well as its absorption feature (seen by HM, but undetected in our data due to our low spectral resolution) and the submillimetric emission (Dunlop et al, 1994) found in this area. Such an absorption feature was also observed and attributed to dust in some of the most distant radiogalaxies, e.g. in the 0943-242 absorbed Lyα profile (Röttgering et al, 1996). The description

of absorption processes, either by dust produced by a massive starburst or by a neutral cloud can be found in van Ojik et al (1994). However, if this absorption traces the inner part of a gaseous/dusty disk seen almost edge on, the real systemic velocity would be that of this component which is blueshifted ($\approx$300 km s^{-1}) relative to the peak at z=3.800.

iv) The highest radial velocities values ($\simeq$-700 km s^{-1}) would locate the frontal bow shocks. But the local emission enhancement is not comparable to the bow shocks of 3C435A (z = 0.37), traced by intense [OII] and [OIII] emission lines (Rocca-Volmerange et al., 1994).

Last, the observed surrounding clouds repartition, although showing no anisotropy evidence, could result from the presence of the ionizing central AGN. Various scenarios may fit these observations, and a detailed analysis of spectra in relation with radio properties and star formation processes is in progress and will take advantage of future deeper spectroscopic observations.

References

Bacon, R., Adam, G., Baranne, A., et al., 1995, A&AS, 113, 347.
Begelman, M.C., Cioffi, D.F., 1989, ApJ, 345, L21.
Blandford, R.D., Rees, M.J., 1974, MNRAS, 169, 395.
Carilli, C. L., Owen, F.N., Harris, D.E., 1994, AJ, 107, 480.
Chambers, K., Miley, G., van Breugel, W., 1990, ApJ, 363, 21.
Chini, R., Krügel, E., 1994, A&A, 288, L33.
Cioffi, D., Blondin, J.M.,1992, ApJ, 392, 458.
Daly, R.A., 1992, ApJ, 399 , 426.
di Serego Alighieri S., Cimatti A., Fosbury R.A.E., 1993, ApJ, 404 , 584.
Dunlop, J., Hughes,D., Rawlings, S., Eales, S., Ward, M., 1994, Nature, 370, 347.
Graham, J.R., Matthews, K., Soifer, B.T., Nelson, J.E., Harrison, W., Jernigan, J.G., Lin, S., Neugebauer, G., Smith, G. and Ziomkovski, C., 1994, ApJ, 420, L5.
Hippelein,H., Meisenheimer,K.,1993, Nature, 362, 224.
HST archive, exposures from proposal 2438, Miley G. et al., 1993.
Lacy M., Rawlings, S., 1996, MNRAS, 280, 888.
Loken C., Burns, J.O., Clarke, D.A., Norman, M.L., 1992, ApJ, 392, 54.
Miley, G., Chambers, K., van Breugel, W., Macchetto, F., 1992, ApJ, 401, L69.
Rocca-Volmerange, B., Adam, G., Ferruit, P., Bacon, R., 1994, A&A, 292, 20.
Röttgering H.J.A., et al., 1996, MNRAS, in press.
Rousset, A., 1992, Thèse, Université J. Monnet, St Etienne, France.
van Breugel, W., Miley, G., Heckman, T., Butcher, H., Bridle, A., 1985, ApJ, 290, 496.
van Ojik, R., Röttgering H.J.A., Miley, G., Bremer, M., Macchetto, F., Chambers, K., 1994, A&A, 289, 54.

This article was processed by the author using Springer-Verlag LaTeX A&A style file *L-AA* version 3.